Buoyancy Effect on the Ultrafiltration of PEG 10,000. Visualization by Digital Holographic Interferometry

Julio Fernández-Sempere, Francisco Ruiz-Beviá, Raquel Salcedo-Díaz, Pedro García-Algado, and Miriam García-Rodríguez
Dept. of Chemical Engineering, University of Alicante, Apartado 99, E-03080 Alicante, Spain

DOI 10.1002/aic.13757
Published online February 15, 2012 in Wiley Online Library (wileyonlinelibrary.com).

Digital holographic interferometry has been used to visualize the buoyancy effects on dead-end ultrafiltration of PEG 10,000. Sets of experiments have been carried out with the membrane in different orientations (90°, 180°), using a feed concentration of PEG 10,000 ranging 5–12.5 kg/m^3. These results were compared with those obtained in previous research with the cell placed in its natural position (0°). The interferometric fringe patterns obtained in this research were very different from those obtained previously. Whereas at the 0° position, an increasing number of interferometric fringes appeared parallel to the membrane surface at 90 and 180° positions, the number of interference fringes was much lesser and, with the 180° orientation, slightly curved protuberances appeared after a short period of time that, like big drops, fell downward from the membrane surface. The consequence is a decrease of the polarization layer and an enhancement of the membrane performance. © 2012 American Institute of Chemical Engineers *AIChE J,* 58: 3810–3817, 2012
Keywords: buoyancy effect, ultrafiltration, PEG 10,000, polarization layer, digital holographic interferometry

Introduction

The main problem with membrane separation processes is the accumulation of solute on the membrane surface, that results in a substantial reduction of the permeate flux. The performance of these pressure-driven membrane processes may be significantly improved when a nonsteady instability of the fluid is superimposed onto the normal flow. One of these phenomena capable of inducing fluid instability near the membrane surface is natural convection.

In reverse osmosis (RO) or ultrafiltration (UF) experiments, the solute accumulated in the polarization layer causes a density distribution in such a way that the solution density at the membrane surface is higher than in the bulk solution. The changing of the gravitational orientation of the membrane causes a density inversion, which may lead to an unstable fluid behavior or "natural convection flow" (buoyancy) in the vicinity of the membrane surface. The effect of this natural convection instability is a displacement of accumulated solutes, moving away from the membrane (depolarizing), that can enhance the membrane performance.

Previous experimental studies carried out in the 70s[1,2] observed the effect of buoyancy on RO. In a more recent article, Ref. 3 studied from a theoretical point of view the effect of buoyancy on the polarization layer in cross-flow RO by simulation with a mathematical model. The simulation was applied to the study of salt water separation in a flat system. In an excellent experimental study on the effects of natural convection instability on membrane performance in dead-end and crossflow UF, the buoyancy phenomenon was presented in a very clear way.[4] According to these authors, who studied a dead-end operation (UF of dextran and bovine serum albumin (BSA) solutions), when using the gravitationally unstable orientation of the cell (180°) the permeate fluxes are enhanced several times: up to 3.5 times for dextran solutions and 5.5 times for BSA solutions compared with the results using the stable orientation (0°). This flux enhancement implies that natural convection flow induced by the density inversion causes a gravitationally unstable state in the concentration boundary layer, which may promote the movement of accumulated solutes away from the membrane surface (depolarizing). During UF at 90° (gravitationally semistable), the fluxes were also enhanced, although less than when the 180° position was used.

In a previous experimental work,[5] real-time holographic interferometry (IH) was used to visualize the buoyancy effects on dead-end RO of salts by rotating the cell 90 and 180° from its original position (0°) (see Figure 1). When the module was in 180° position, great instabilities were observed in the polarization layer due the natural convection currents caused by the density gradient. Some material moving downward from the membrane surface was observed, similar to the jets described in Ref. [1]. The main consequence of the buoyancy effect is a great enhancement of the membrane performance and, therefore, a higher effectiveness of the RO process.

According to the results described in the articles previously cited, the best way to study the effects of buoyancy is working in dead-end conditions. Working in cross-flow conditions, gravitational effects, which was observed, were only important at low flow rates because high velocities may overshadow the effect of natural convection.[3] These authors

Correspondence concerning this article should be addressed to F. Ruiz-Beviá at ruiz.bevia@ua.es.

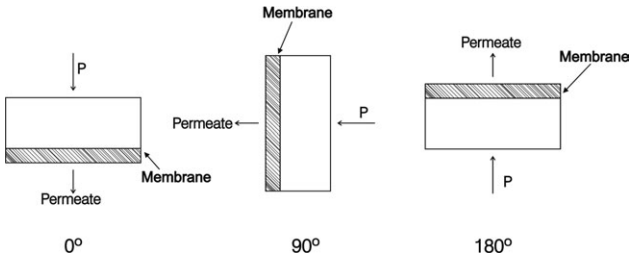

Figure 1. Schematic diagram of the three positions of the module.

used four different inlet velocities (0.002, 0.005, 0.01, and 0.1 m/s, corresponding to Re numbers ranging from 8 to 400) in the computational fluid dynamics study of buoyancy effects in RO. Results of permeate flow showed that the effect of buoyancy was only significant when the lowest inlet velocity (Re = 8) was used. On the other hand, according to Ref. 4, when dextran and BSA solutions are ultrafiltered, permeate flux enhancements by natural convection instability only occurs if the cross-flow velocity is lower than 0.1–0.2 m/s (Re = 35–90).

The aim of this work, as a continuation and a complement to the previous RO research,[5] is to visualize and study the buoyancy effects on an UF process. Thus, besides studying in UF processes, the buoyancy effect on the permeate flux in Ref. 4, it is intended to visualize the polarization layer while the buoyancy phenomenon occurs. The experimental technique used is digital holographic interferometry (DHI), a variation of the conventional HI technique previously used to study diffusion in transparent media,[6,7] the concentration polarization phenomenon when ultrafiltering BSA[8] and buoyancy effects in a RO process,[5] the main difference of which is the recording element. In classical HI, a holographic plate, photographically developed, is used. In DHI, the holographic plate is substituted by the CCD chip of a video camera. The digital technique is as valid as the classical one and has also been used in diffusion studies[9–11] and in the experimental study of the concentration polarization in a crossflow RO system.[12]

In the present research, to determine the effects of instabilities due to natural convection on dead-end UF processes, several experiments were carried out changing the gravitational orientation of the module: horizontal but placing the membrane at the top (gravity acting in the opposite direction to the flow) which is the most gravitationally unstable orientation (180°) and vertical, with zero gravity perpendicular to the flow direction (90°). Experiments were carried out using PEG 10,000 solutions. Results with the 0° orientation were obtained in a previous article[13] and have been compared with those obtained with 90 and 180° orientation in this research.

According to the previous study,[13] the phenomena occurring on the surface of the membrane in UF are different from those taking place in RO. In dead-end RO, the accumulated salts in the polarization layer are dissolved and match the amount of solute received by the membrane by convective flow. In dead-end UF, only part of the macromolecules that reach the vicinity of the membrane remain dissolved in the polarization layer, whereas another important part of them is retained on the membrane surface. Then, the behavior of the instabilities during UF processes is expected to be different from that observed in the research about buoyancy in RO processes.[5]

Experimental

Experimental set-up

Two different systems are linked together in the experimental assembly: the optical set-up for the DHI and the UF system. These two assemblies were coupled on the same working table, with the UF module as the common element.

The DHI set-up used was the same as that previously described when studying the RO process.[12] The UF system was the same as previously used,[13] with an UF cell thoroughly described in a previous article.[14] The cell was designed to satisfy the interferometric requirements. The active membrane area was 10 cm^2 (10 cm × 1 cm), whereas the distance from the membrane surface to the top of the cell was 40 mm, so the volume of solution in the cell was large enough to guarantee that the bulk concentration remained constant during the process and the concentration changes inside the cell would only take place near the membrane surface. Throughout the research, the UF cell was rotated to obtain different gravitational orientations: horizontally placed with the membrane surface facing downward (180°) and vertically placed (90°).

Materials and experimental procedure

In this research, two sets of experiments (90 and 180°) were carried out using solutions of PEG 10,000 (Sigma) with different initial concentration (C_o), in the range from 5 to 12.5 kg/m^3. Both of them were performed in batch conditions using a constant pressure of 1 bar and a cellulose acetate membrane, YC05 from Millipore, with nominal molecular weight limit (NMWL) 500. Before each experiment, water flow (J_w) was measured to verify that it had not decreased very much, thus indicating that the membrane was still in good condition.

The experimental procedure was very similar to that used in the previous work.[13] The main difference in the experimental methodology was the way to obtain the reference state for the interferometry. Whereas in the previous article, classical HI was used, and it was necessary to record the reference state in the holographic plate, in this research, the hologram has been recorded in the CCD chip. Then, with the solution at rest and the optical set-up correctly aligned, the hologram capture program was started. The video camera captures the images (at a rate of 1/s) and sends them to the PC, thus beginning the calculation of the interferograms. Afterward, pressure was applied and the process started. The reference state (the hologram) for the interferometric process was the first image captured by the camera, before the process had started and any change had undergone inside the cell.

Data of the evolution of the permeate weight were taken during the experiment to calculate the permeate flux. Several permeate samples were also collected to measure the concentrate of the permeate (C_p). After 2 h 15 min of experiment, the pressure was removed and the convective flux of solute to the membrane ceased. The capture of the images continued for 15 min after stopping the process to follow the evolution of the polarization layer once the pressure ceased.

Results and Discussion

Visualization of the polarization layer and buoyancy effects in the vicinity of the membrane

Really, as later will be stated, a completely developed polarization layer only exists in the 0° gravitational

Table 1. Experiments Carried Out

Experiment	Cell orientation	C_o (kg/m^3)	$J_w \times 10^6$ (m^3/m^{2}s)	$R_m \times 10^{-10}$ (Pa s/m)
I	90°	5	2.57	3.89
II		7.5	2.61	3.83
III		10	2.61	3.83
IV		12.5	2.60	3.85
V	180°	5	2.95	3.39
VI		7.5	2.92	3.43
VII		10	2.96	3.38
VIII		12.5	2.96	3.38

orientation. In a previous article,[13] a set of experiments were carried out with the UF cell in a horizontal unstirred batch cell, placing the membrane at the bottom (gravity acting in the same direction as the flow direction, orientation 0°). In this work, using the same experimental procedure, except for the use of DHI instead of classical HI, two new sets of experiments were carried out, each one with the UF cell in a different gravitational orientation (180 and 90°) (see Figure 1). For each orientation of the membrane, solutions with different concentrations of PEG 10,000 were used. Experimental conditions are shown in Table 1, where C_o is the bulk concentration, J_w is the permeate flux for pure water, and R_m is the membrane hydraulic resistance to the flux with pure water, which is calculated as

$$R_m = \Delta P / J_w \quad (1)$$

Orientation 0°

To better understand the effect of the buoyancy on the polarization layer, a brief summary of the results obtained in a previous article with orientation 0° [13] is shown here. Using real-time holographic interferometry in a module with this gravitational orientation, the appearance, evolution and disappearance of the polarization layer was visualized as interference fringes. As an example, some interferograms corresponding to two experiments with different initial concentrations of PEG 10,000 (7.5 and 12.5 kg/m^3) were shown to illustrate the evolution of the polarization layer. For comparative purposes, two interferograms corresponding to the experiment with 12.5 kg/m^3 (at 900 and 3600 s) are presented in Figure 2. In each interferogram, a horizontal line and an auxiliary scale have been drawn to show where the membrane surface was initially as well as the magnification used in the experiment.

As the experiments were recorded in a continuous way, a great number of interferograms were available. Video 1 in the same article,[13] (http://www.ua.es/es/servicios/si/servicios/videostreaming/iq/UF_PEG_video1.html) showed the whole experiment (60 min) corresponding to an initial concentration of 12.5 kg/m^3. The speed in the video was increased 60 times, so the video was 1 min long (1 min of experiment = 1 s of video). As can be seen in the video, a few minutes after the UF process started, some parallel interferometric fringes near the membrane surface appeared. The amount of fringes continued increasing throughout the process, thus indicating that the concentration at the membrane surface (C_m) was increasing, as well as the thickness of the boundary layer (δ).

As it was already seen, the behavior in these UF experiments contrasts with that observed when RO experiments were carried out.[15] In the RO experiments, the amount of solute retained by the membrane in the polarization layer (calculated from the area under the curve concentration–distance) was very similar to the total mass of solute that had entered in the boundary layer by convection during the filtration period. However, in UF the amount of incoming solute was greater than the solute retained in the polarization layer. These experimental results indicate that part of the solute transported by convection to the membrane did not remain dissolved in the polarization layer but was deposited on the membrane surface. This phenomenon of PEG macromolecules deposited on the membrane can be explained in two ways. It may be due to either a reversible adsorption process on the membrane or the fact that PEG solution reaches some type of concentration limited condition (e.g., gel layer formation). In the literature on membrane processes is widely accepted that PEG is a nonadsorptive, nonfouling solute. However, some authors do admit phenomena of reversible adsorption of PEG macromolecules onto membranes. For instance, Ref. 16 in a article entitled "*Reversible adsorption inside pores of ultrafiltration membranes*" textually states; "*In accordance with experimental observations, it is assumed below that adsorption of PEG molecules inside membrane pores is reversible*". More recently in 2011, an article have been published with experiments carried out using PEG in static and dynamic adsorption conditions, noting that the adsorption increases with the applied pressure.[17] The elucidation of the true mechanism of PEG deposition would require conducting independent experiments to test if PEG solute is truly adsorbed or not. Whatever the mechanism (adsorption or formation of a deposit when a limited concentration condition is reached), the process is reversible, as is shown in the experiments presented below.

Once pressure ceased, the almost immediate appearance of a high number of new fringes was observed, nearly twice as many as there were before removing the pressure. Afterward, the number of interference fringes decreased as time went on, they became wider and the thickness of the boundary layer increased. This process can be seen in the Video 2 (http://www.ua.es/es/servicios/si/servicios/videostreaming/iq/UF_PEG_video2.html) and in Figure 7 published in a previous article.[13] During this process, the evolution of interference fringes also showed differences between the UF and RO experiments.[15] In RO, there was no appearance of new fringes; the fringes became wider and slowly disappeared. This phenomenon was due to the diffusive movement of the solute accumulated in the polarization boundary layer during the process, from the solution closest to the membrane

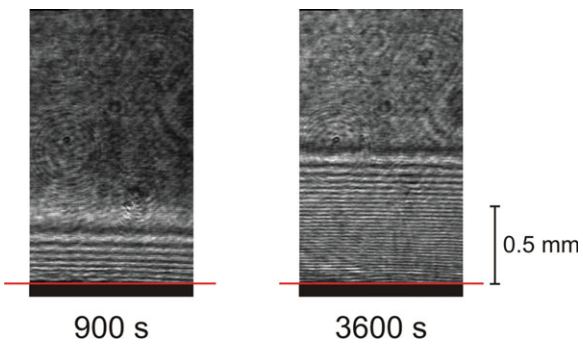

Figure 2. Interferograms at 900 and 3600 s of the UF experiment with 0° Orientation (C_o = 12.5 kg/m^3).[13]

[Color figure can be viewed in the online issue, which is available at wileyonlinelibrary.com.]

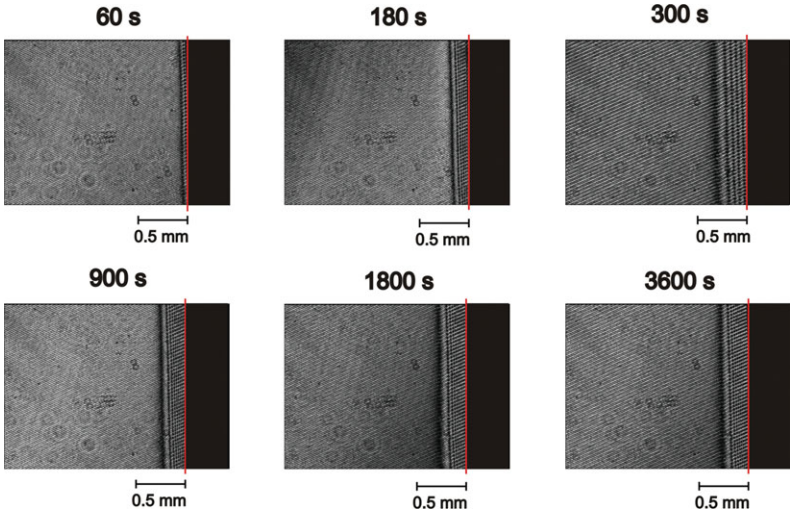

Figure 3. Interferograms of experiment IV, with 90° Orientation and C_o =12.5 kg/m^3.

[Color figure can be viewed in the online issue, which is available at wileyonlinelibrary.com.]

surface to the bulk solution. In UF, the appearance of new fringes and the later disappearance of all of them could be the consequence of the combination of two phenomena: the release process of the solute deposited and the diffusion of solute back to the solution. During the first few minutes, the predominant mechanism was the release of the solute layer on the membrane surface. As time went on, the solute provided from the membrane became lesser than the solute that went back to the bulk solution by diffusion and the number of interference fringes decreased with time as the diffusion progressed and the solute was incorporated to the bulk solution.

In summary, it is evident that mechanisms that explain the phenomena occurring on the membrane surface in UF are different from those taking place in RO.

Orientation 90°

With this orientation of the module (zero gravity acting perpendicular to the flow direction), the evolution of the polarization layer is slightly different to that observed with the orientation 0° as a consequence of the buoyancy effect. However, this phenomenon is not as noticeable as in the orientation 180°, as will be later explained. Video 3 (http://hdl.handle.net/10045/18952), shows the first 3 min at the beginning of experiment IV with 12.5 kg/m^3 initial concentration of PEG 10,000, with the module in vertical orientation. To better visualize the changes that occur, the video reproduces the images at three times the speed of the real process (as a consequence, the video is 60-s long). In addition, Figure 3 shows interferograms at 60, 180, 300, 900, 1800, and 3600 s corresponding to the same experiment.

At the beginning of the process, a few interference fringes parallel to the membrane surface appeared which indicate that a concentration profile, similar to that obtained at 0° position, had been developed. However, whereas at 0° new interference fringes continuously appeared during the process, at 90° only few fringes (from eight to eleven, depending on the concentration used) appeared during the first 15 min, and then the concentration profile became stable for a long period of time (about 2 h in most of the experiments). The polarization layer thickness (δ) behaved in a similar way: at the position 0°, it grew continuously with time, reaching almost 1 mm, whereas at 90°, the thickness of the polarization layer was minor (only 0.3–0.4 mm) and stable.

According to these results, the dead-end UF process with the membrane vertically placed (90°) seems to reach a steady-state. The convective flow towards the membrane is balanced by the buoyancy effect, i.e., by the removal of solute near the membrane by natural convection. Otherwise, the batch process with the horizontal membrane facing upward (0°) is unsteady due to the continuous contribution of convective flow of solute toward the membrane.

Once pressure was removed, the interference fringes first underwent slight slow changes and afterwards they disappear. Video 4 (http://hdl.handle.net/10045/18953) shows the first 15 min after the pressure ceased in experiment IV. The speed in the video was increased 15 times, so the video was 1 min long. Moreover, Figure 4 shows interferograms at 30, 60, 120, 300, 600, and 900 s corresponding to the same experiment. As can be observed, during the first seconds after removing the pressure, the number of interference fringes remains almost constant (around 12) although a small widening of the fringes and a slight increase of the polarization layer thickness (δ) (see interferogram at 60 s) is observed. This evolution continues for a few minutes and, after that, there is a decrease in the number of fringes. Then, at 300 s (see interferogram), the number of fringes has been reduced to 5–6 and they are wider; later, at 1800 s, no interference fringes were visible, thus indicating that the concentration gradient had disappeared and the solution into the module was homogenized.

The period needed to the disappearance of the fringes with the 90° orientation is very different to that observed with the 0° orientation. With this latter orientation, after 50 min there were still a great number of fringes (up to 40 fringes, see Figure 7, in Ref. 13) as a result of the combination of two processes: the slow diffusion of the high amount of solute accumulated in the polarization layer and the return of the solute retained or adsorbed on the membrane. In contrast, with the 90° orientation, the number of interference fringes is less (less amount of solute in the polarization layer), the diffusion process is enhanced by the natural convection and the period of time needed to the homogenization of the solution decreases. When the

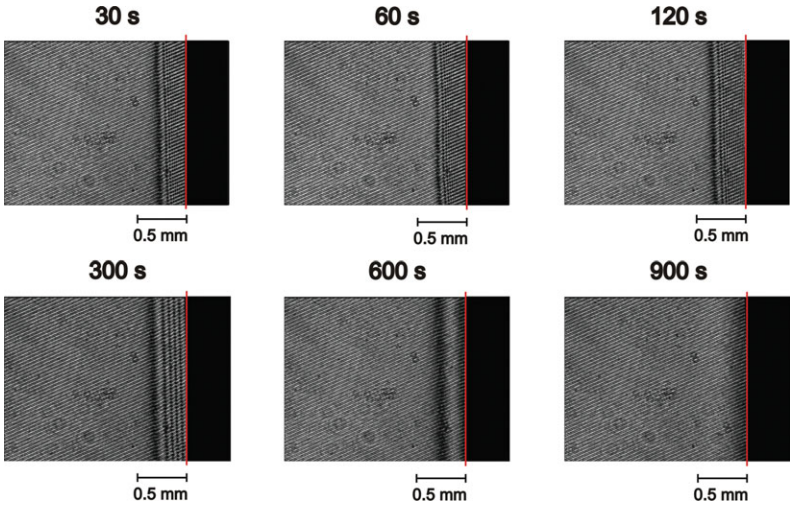

Figure 4. Interferograms of experiment IV, with 90° Orientation and C_o =12.5 kg/m^3, after the pressure ceased.

[Color figure can be viewed in the online issue, which is available at wileyonlinelibrary.com.]

concentration changes, the behavior is similar, being the effect more accentuated for the greatest concentration.

Orientation 180°

This orientation of the cell, with gravity acting in the opposite direction to the flow, is the most gravitationally unstable orientation, where natural convection or buoyancy flow in the vicinity of the membrane surface is produced. The real-time holographic interferometry technique allows the gravitational effects on the boundary layer near the membrane to be visualized. Video 5 (http://hdl.handle.net/10045/18954), shows the first 3 min at the beginning of experiment VIII, with a feed concentration of 12.5 kg/m^3 of PEG 10,000. The video reproduces the images at three times the speed of the real process and, consequently, the video is 1-min long. In addition, Figure 5 shows interferograms at 55, 110, 120, 180, 1800, and 3600 s corresponding to the same experiment.

In this case, the fringe patterns were also different from those obtained when the module was in the 0° orientation. Instead of a concentration profile continuously increasing, after the cell was pressurized only a few fringes (from 3 to 5 depending on C_o), parallel and very close to the membrane, began to appear. A few seconds later, the fringes, especially those farthest from the membrane (see interferogram at 105 s), ceased to be straight lines, lost their parallel to the membrane surface shape, and slightly curved protuberances appeared. These small protuberances grew slowly and became something with a shape like big drops or elongated fluctuating blobs, moving downward from the membrane surface. This process is continuously repeated in a cyclical way, so that the fringe that was transformed and disappeared is replaced by a new one which also undergoes the subsequent deformation: small protuberances first and then the big drops moving downward. The same behavior was observed during all the process (see interferogram at 3600 s), i.e., an area close to the membrane with scarce fringes and another area with a continuous shower of elongated fluctuating blobs starting from the last fringe.

This behavior was similar to that described by the authors[5] when studying the buoyancy effects in a dead-end RO process. However, there are some differences in the intensity and thickness of the blobs moving downward from the membrane surface, larger in UF than in RO. A possible explanation for this difference between RO and UF in the effect of the phenomenon of buoyancy could be the different mechanism of formation of the polarization layer in RO and UF above mentioned (see Orientation 0°). In the RO process, there is only an accumulation of dissolved salts in the vicinity of the membrane surface, and the variation of solute concentration (i.e., a variation of the solution density) leads to a fluid instability in this membrane position. In the UF process, besides the accumulation of dissolved macromolecules in the polarization layer (that causes a density gradient as in the RO), should be added the mass accumulation of deposited macromolecules on the membrane. With the module in the orientation 0°, the macromolecules would be reversibly retained or adsorbed on the membrane but with this 180° orientation, accumulation is unstable and thus the blobs are more gravitationally affected. Furthermore, due to the higher viscosity of the solution of PEG macromolecules compared with a solution of inorganic salts, the blobs formed during UF fall slower than those formed in RO. This effect can be better understood by comparing Video 5 presented in this article with the video on the RO process (http://www.ua.es/es/servicios/si/servicios/videostreaming/iq/Video1.html), already published.[5]

When pressure was removed, the convective solute flux to the membrane surface ceased and, at the beginning, some perturbations could be observed as a consequence of the pressure stopping. The fringe pattern changed and showed a tendency to form new fringes parallel to the membrane surface. Video 6 (http://hdl.handle.net/10045/18955) shows the first 15 min after the pressure ceased in experiment VIII. The speed in the video was increased 15 times, so the video was 1 min long. In addition, Figure 6 shows interferograms at 26, 32, 40, 60, 120, and 600 s, corresponding to the same experiment. Once pressure ceased, the behavior of the UF process with the module orientation 180° was again very different from that with orientation 0°. The main differences are the number of new fringes that appeared and the time needed to restore the homogeneity of solute concentration in the bulk solution.

With regard to the number of fringes, with orientation 0° the number of fringes that appeared was numerous (40–50), greater than before ceasing the pressure. As was stated, this

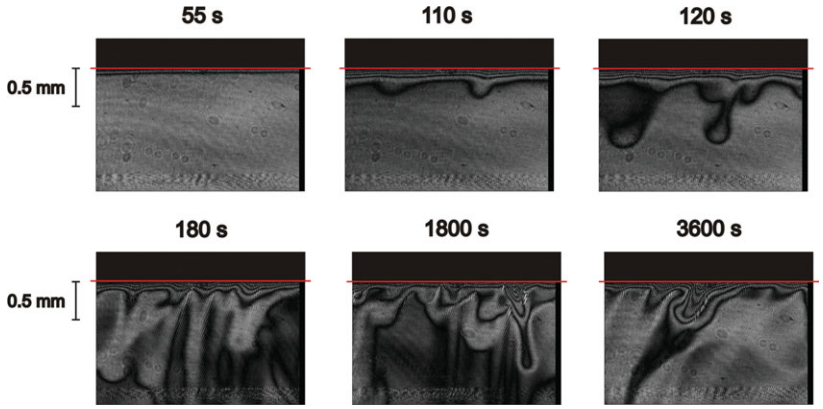

Figure 5. Interferograms of experiment VIII, with 180° Orientation and C_o =12.5 kg/m^3.

[Color figure can be viewed in the online issue, which is available at wileyonlinelibrary.com.]

increase could be attributed to the return to the solution of the macromolecules deposited in the membrane by a reversible mechanism. When the 180° orientation was used, the number of fringes also increased, but less than with the 0° orientation (the total number of new fringes was around 7). In this case, due to the buoyancy effect, during the UF process, the accumulation of macromolecules on the membrane is reduced.

With regard to the time of the disappearance of the fringes, indicating a solute concentration gradient in the vicinity of the membrane, in the case of orientation 0°, it was relatively high (after 50 min there still existed a large number of fringes in a polarization layer of more than 2 mm, almost twice the thickness than before ceasing pressure). This slow disappearance of the concentration profile in the module can be explained considering that only the slow diffusion process is involved. However, with the orientation 180°, the prevailing buoyancy process accelerated the disappearance of the fringes and the homogeneity of the concentration. As can be seen in the interferogram at 300 s of Figure 6, there are only two fringes.

Experiments with the 180° orientation show qualitatively similar results regardless of the initial concentration. However, due to the viscosity, which varies depending on the concentration of the experiment, small differences exist in the behavior of the polarization layer. The high viscosity of the solution of macromolecules hinders the dripping of solute and, consequently, a higher concentration difference is needed to reach such a density difference to create a gravitational unstable state. Figure 7 shows some interferograms of experiment V, with 5 kg/m^3 of initial concentration with this orientation. In the figure, a smaller number of fringes can be observed (only 1-2), compared to experiment VIII, i.e., the polarization layer built up in experiment V is less than in experiment VIII. This phenomenon is because the higher the C_o, the greater its viscosity. Therefore, with the higher concentration, more fringes appear (more polarization layer) due to the greater concentration difference needed to lead to the unstable state. As an example, videos 7, 8, and 9 show the first 3 min at the beginning of the experiment as well as the first 6 min after the pressure ceased in experiments V, VI, and VII. Videos show the beginning with three times the speed of the real process, whereas after the pressure ceases the speed increases to six times. As a consequence, the videos are 2-min long.

- Video 7: http://hdl.handle.net/10045/18956 ($C_o = 5$ kg/m^3)
- Video 8: http://hdl.handle.net/10045/18957 ($C_o = 7.5$ kg/m^3)
- Video 9: http://hdl.handle.net/10045/18958 ($C_o = 10$ kg/m^3)

Membrane performance

In all the experiments developed, permeate flux (J) and concentration of the permeate solution (C_p) were measured. Both are important parameters to quantify the membrane performance and, therefore, the process effectiveness. The concentration of the permeate solution was found to be nearly 0, indicating almost complete rejection of the solute. This result was expected due to the high difference between

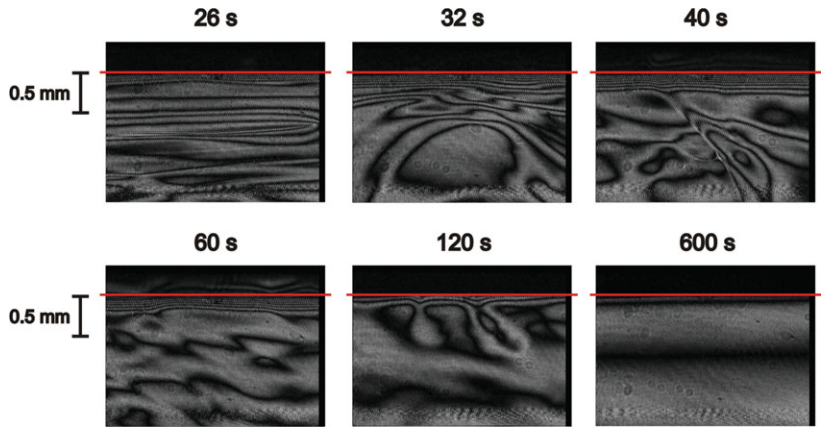

Figure 6. Interferograms of experiment VIII, with 180° Orientation and C_o =12.5 kg/m^3, after the pressure ceased.

[Color figure can be viewed in the online issue, which is available at wileyonlinelibrary.com.]

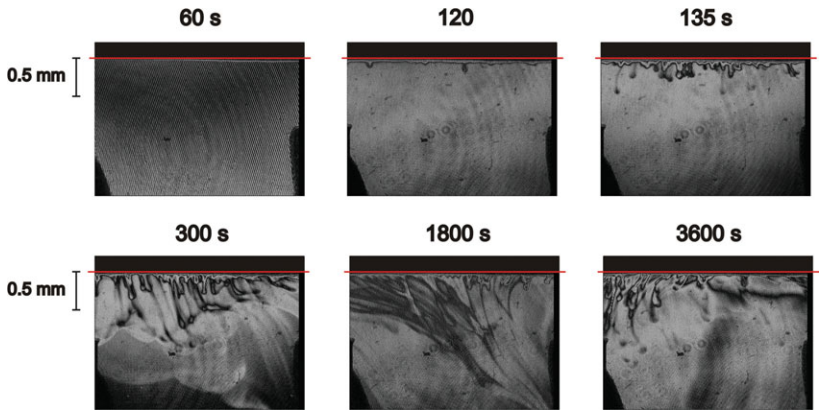

Figure 7. Interferograms of experiment V, with 180° Orientation and C_o = 5 kg/m^3.

[Color figure can be viewed in the online issue, which is available at wileyonlinelibrary.com.]

the NMWL of the membrane (500) and the molecular weight of the solute (10,000).

As dead-end UF is an unsteady state process, J changes continuously. The reduction of the permeate flux related to pure water flux (J_w) has been calculated. Data of J_w are presented in Table 1 and Figures 8 and 9 show the non-dimensional J/J_w curves corresponding to the orientations 90 and 180° for each concentration (5, 7.5, 10, 12.5 kg/m^3). Figure 10 shows the permeate flux curves for the experiment with 12.5 kg/m^3 and each orientation used. Data corresponding to the orientation 0° have been taken from a previous article.[13]

The reduction of permeate flux was much higher at 0° than at 90 and 180°. As can be appreciated in the above-mentioned Figures, the gravitational orientation of the UF module had a great effect on the evolution of the permeate flux. Then, an important increase in the permeated flux was obtained when positions 90 and 180° were used. At the 0° position,[13] the evolution of the experimental dimensionless flux for each feed concentration, had the typical shape of the permeate flux curves. During the first minutes of the process, a great reduction occurred, and later the flux decreased more slowly.

At the other two positions (90 and 180°), the permeate flux underwent a continuous but smooth reduction during the entire process. In these two positions, the shape of the permeate flux curves was nearly linear. Not only the shape of the curves but also the values of the permeate flux were different between the 0° position and the other two. This difference between the values of the permeate flux is a consequence of the different behavior of the solution in the vicinity of the membrane, depending on its position. The polarization layer that grew when the membrane was facing upwards (0°) produced an increase in the osmotic pressure of the solution, which caused a decrease in the driving force of the process ($\Delta P - \pi$) and, therefore, in the permeate flux. The flow instability induced when the membrane was placed vertically and horizontally facing downward (90 and 180°) caused a buoyancy flow that tended to destroy the polarization layer. Then, the decrease in the driving force was not so high and the flux reduction was less. Moreover, in these two positions, the accumulation of solute by a reversible mechanism on the membrane surface is very unstable, which also contributes to a low reduction in the permeate flux. These results are very similar to those presented in Ref. 4 in which an important enhancement was obtained in the permeate flux when the cell was placed in an unstable gravitational orientation. Therefore, the research confirms that the buoyancy effect improves the performance of membrane processes, and that DHI is a useful optical technique to visualize the phenomena occurring in the vicinity of the membrane.

Conclusions

DHI, an optical technique, has been successfully used to visualize the buoyancy effects on dead-end UF of PEG

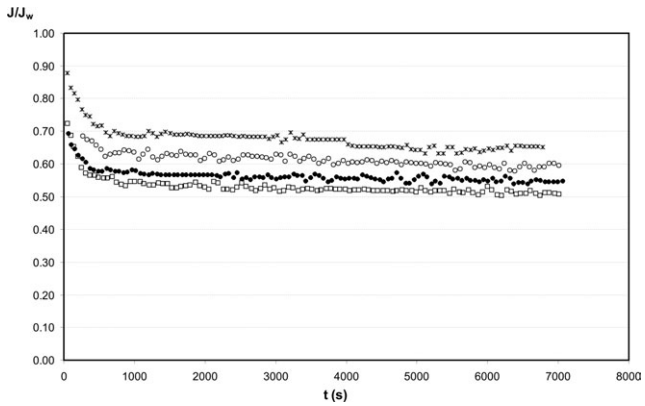

Figure 8. Permeate flux related to pure water for each feed concentration, with 90° Orientation (x: 5 kg/m^3; ○: 7.5 kg/m^3; ●: 10 kg/m^3; □: 12.5 kg/m^3).

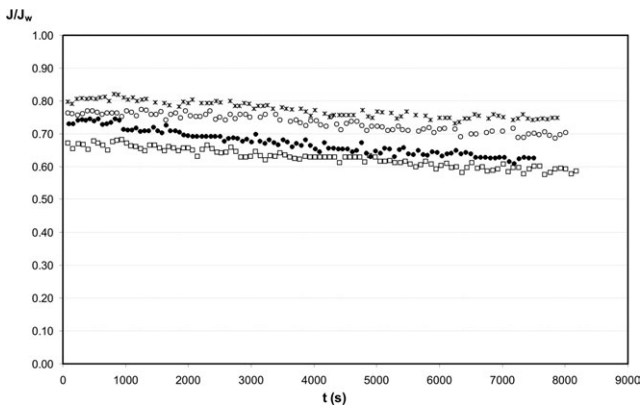

Figure 9. Permeate flux related to pure water for each feed concentration, with 180° Orientation (x: 5 kg/m^3; ○: 7.5 kg/m^3; ●: 10 kg/m^3; □: 12.5 kg/m^3).

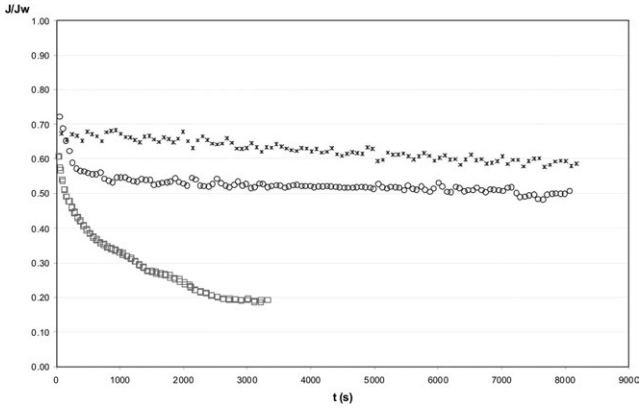

Figure 10. Permeate flux related to pure water for each orientation used and C_o = 12.5 kg/m^3 (x: 180°; ○: 90°; □: 0°).

10,000, by changing the gravitational orientation of the cell (90 and 180°). The gravitational orientation of the UF module has a great effect on the evolution of the permeate flux. The shape of the flux and rejection curves when positions 90 and 180° were used is very different from those obtained for the 0° position. Furthermore, values obtained of flux and rejection are also higher in the positions where buoyancy flow was induced (90 and 180°).

The behavior observed during the UF process is similar to that previously described[5] when studying the buoyancy effects in a RO process. However, the intensity and thickness of the blobs moving downward from the membrane surface are different, larger in UF than in RO. The explanation could be the different mechanism of formation of the polarization layer in RO and UF. In RO, there is only an accumulation of salts near the membrane surface and the variation of the solution density causes a fluid instability. In UF, besides a density gradient as in RO, there is a mass accumulation of deposited macromolecules on the membrane. Furthermore, as the viscosity of the PEG solution is higher than that of the solution of inorganic salts, the dripping of solute is hindered and it is more difficult to reach an unstable state. Therefore, in the UF experiments, greater polarization layer appeared. Moreover, due also to viscosity, the blobs formed during UF fall more slowly than those formed in RO.

The results of this research prove the existence of a buoyancy effect in dead-end UF of PEG 10,000, depending on the gravitational orientation of the membrane surface. The consequence of this phenomenon is a great enhancement of the membrane performance and, therefore, a higher effectiveness of the UF process.

Acknowledgements

This research has been sponsored by the Plan Nacional de I+D+i CTQ2009-14109 (Ministerio de Ciencia e Innovación).

Literature Cited

1. Hendricks TJ, Macquin JF, Williams FA. Observations on buoyant convection in reverse osmosis. *Ing Eng Chem Fundam*. 1972;11:276–279.
2. Derzansk L, Gill WN. The mechanisms of brine-side mass transfer in a horizontal tubular membrane. *AIChE J*. 1974;20:751–761.
3. Fletcher DF, Wiley DE. A computational fluids dynamics study of buoyancy effects in reverse osmosis. *J Membr Sci*. 2004;245:175–181.
4. Youm KH, Fane AG, Wiley DE. Effects of natural convection instability on membrane performance in dead-end and cross-flow ultrafiltration. *J Membr Sci*. 1996;116:229–241.
5. Fernández-Sempere J, Ruiz-Beviá F, Salcedo-Díaz R and García-Algado P. Buoyancy effects in dead-end reverse osmosis. Visualization by holographic interferometry. *Ind Eng Chem Res*. 2007;46:1794–1802.
6. Ruiz-Beviá F, Fernández-Sempere J, Colom-Valiente J. Diffusivity measurements in calcium alginate gel by holographic interferometry. *AIChE J*. 1989;35:1895–1898.
7. Ruiz-Beviá F, Fernández-Sempere J, Boluda-Botella N. Variation of Phosphoric acid difusión coeficiente with concentration. *AIChE J*. 1995;41:185–189.
8. Fernández-Torres MJ, Ruiz-Beviá F, Fernández-Sempere J, López-Leiva M. Visualization of the UF polarized layer by holographic interferometry. *AIChE J*. 1998;44:1765–1776.
9. Anand A, Chhaniwal VK, Narayanamurthy CS. Diffusivity studies of transparent liquids solutions by use of digital holographic interferometry. *Appl Opt*. 2006; 45:904–909.
10. Richter J, Leuchter A, Großer N. Digital image holography for diffusion measurements in molten salts and ionic liquids – Methods and first results. *J Mol Liq*. 2003;103–104:359–370.
11. Wylock C, Dehaeck S, Cartage T, Colinet P, Haut B. Experimental study of gas-liquid mass transfer coupled with chemical reactions by digital holographic interferometry. *Chem Eng Sci*. 2011;66:3400–3412.
12. Fernández-Sempere J, Ruiz-Beviá F, García-Algado P, Salcedo-Díaz R. Experimental study of concentration polarization in a crossflow reverse osmosis system using digital holographic interferometry. *Desalination* 2010;257:36–45.
13. Fernández-Sempere J, Ruiz-Beviá F, García-Algado P, Salcedo-Díaz R. Visualization and modelling of the polarization layer and a reversible adsorption process in PEG-10000 dead-end ultrafiltration. *J Membr Sci*. 2009;342:279–290.
14. Fernández-Sempere J, Ruiz-Beviá F, Salcedo-Díaz R, García-Algado P. Equipo experimental para visualizar la formación de la capa de polarización durante el proceso de ósmosis inversa. *Ing Quim*. 2006;438:147–154.
15. Ruiz-Beviá F, Fernández-Sempere J, Salcedo-Díaz R, García-Algado P. Measurements of concentration profiles by holographic interferometry and modeling in unstirred batch reverse osmosis. *Ind Eng Chem Res*. 2006;45:7219–7231.
16. Churaev NV, Holdich RG, Prokopovich PP, Starov VM, Vasin SI. Reversible adsorption inside pores of ultrafiltration membranes. *J Colloid Interface Sci*. 2005;288:205–212.
17. Li L, Szewczykowski P, Clausen LD, Hansen KM, Jonsson GE, Ndoni S. Ultrafiltration by gyroid nanoporous polymer membranes. *J Membr Sci*. 2011;384:126–135.

Manuscript received Oct. 13, 2011, and revision received Dec. 16, 2011.